NUMERICAL SIMULATION OF TURBULENT ENVIRONMENTAL FLOWS

Jucá, P.C.S. and Maliska, C.R.
Computational Fluid Dynamics Laboratory - SINMEC
Department of Mechanical Engineering - UFSC
88040-900 - Florianópolis - SC - Brazil

INTRODUCTION

Water is one of the most basic resource used by the human being and since the antiquity has influenced the geographical location of the ancient human agglomerates. To maintain the quality of the water in closed water bodies is a delicate issue due to their limited capacity in assimilating and dispersing the pollutants disposed in it by direct (e.g. waste waters) or indirect actions (e.g. agriculture chemicals carried by rain) of local populations. In studying the effects of any kind of water pollution in closed water bodies the knowledge of its hydrodynamic behavior is of utmost importance. This is one of the most determining factor in the capacity of the water body in assimilating and dispersing any pollutant. For a lake, for example, the hydrodynamic pattern is basically determined by the wind currents acting over its surface. The surface of a lake in a wind day shows surface waves that move toward the wind direction and transport a large amount of energy. However, this waves causes a very little transport of mass due to the oscillatory motion, since particles in waves actually moves in orbits. So, when bulk mass transport must be considered, the wave motion is not of fundamental importance. The shear stress, in the other hand, acting in the surface due the wind motion causes a turbulent movement that is not of oscillatory nature and is quite steady, the so called wind driven currents. Therefore, numerical models able to predict the flow pattern in closed water bodies such channels, lakes and lagoons are very useful tool for environmental studies in such sites. In this paper it is reported the simulation of turbulent wind driven flows in closed water bodies. The main goal is validate the mathematical model using a laminar and a turbulent analytical solution for comparison.

THE MATHEMATICAL MODEL

This class of flow is ruled by the Navier-Stokes equations, the mass conservation equation and a turbulence model to describe the turbulent nature of the motion. Using ϕ to represent any of the dependent variables, a general conservation equation can be written as

$$\frac{1}{J}\frac{\partial(\rho\phi)}{\partial t} + \frac{\partial}{\partial\xi}(\rho U\phi) + \frac{\partial}{\partial\eta}(\rho V\phi) + \frac{\partial}{\partial\gamma}(\rho W\phi) = -\hat{P}^{\phi} + \hat{S}^{\phi}$$
$$+ \frac{\partial}{\partial\xi}\left[\left(\alpha_{11} J\Gamma\frac{\partial\phi}{\partial\xi}\right) + \left(\alpha_{12} J\Gamma\frac{\partial\phi}{\partial\eta}\right) + \left(\alpha_{13} J\Gamma\frac{\partial\phi}{\partial\gamma}\right)\right]$$
$$+ \frac{\partial}{\partial\eta}\left[\left(\alpha_{21} J\Gamma\frac{\partial\phi}{\partial\xi}\right) + \left(\alpha_{22} J\Gamma\frac{\partial\phi}{\partial\eta}\right) + \left(\alpha_{23} J\Gamma\frac{\partial\phi}{\partial\gamma}\right)\right] \tag{1}$$
$$+ \frac{\partial}{\partial\gamma}\left[\left(\alpha_{31} J\Gamma\frac{\partial\phi}{\partial\xi}\right) + \left(\alpha_{32} J\Gamma\frac{\partial\phi}{\partial\eta}\right) + \left(\alpha_{33} J\Gamma\frac{\partial\phi}{\partial\gamma}\right)\right]$$

where, due to the irregular shapes of water bodies, a general body-fitted curvilinear coordinate system is employed. If an structured grid is used, as in this work, the boundary conditions for the governing equations are easily imposed using this type of coordinate systems. In Eq.(1) U,V,W are the contravariant components of the velocity vector given by

$$U = (u_1\xi_x + u_2\xi_y + u_3\xi_z)\,J^{-1}$$
$$V = (u_1\eta_x + u_2\eta_y + u_3\eta_z)\,J^{-1} \tag{2}$$
$$W = (u_1\gamma_x + u_2\gamma_y + u_3\gamma_z)\,J^{-1}$$

where J is the jacobian of the coordinate transformation and u_1, u_2, u_3. The right hand side contains the pressure source and the diffusion terms. The contravariant velocity components are responsible for the advection across coordinate lines. As stated, ϕ represents the dependent variables for each equation. For ϕ = 1, u_1, u_2, u_3, the mass conservation equation, momentum in x, y and z, are recovered, respectively. Γ represents the diffusivity transport coefficient, being zero for the mass conservation equation and equals to the effective viscosity (μ_{ef}) for the Navier-Stokes equations. Also in Eq. (2) u_i (i= 1,2,3) represents the mean of fluctuating Cartesian velocities as defined by Rodi [1]. The expressions for P^{ϕ} and for the source terms S^{ϕ} can be fund in Jucá and Maliska [7] and details of coordinate transformation in Maliska [2]

Eq. (1), representing the system of partial differential equations governing the flow, is integrated in time and in a 3D elemental control volume. The pressure-velocity coupling is handled using the SIMPLEC method of Van Doormaal and Raithby [3]. Fictitious control volumes are used for the application of the boundary conditions. Due to the 3D nature of the problem, numerical details and expressions of the coefficients are not given here. These can be found in Jucá [4] and Maliska [2]. To deal with turbulent flows a turbulence model is implemented and will be discussed in detail later. In the Navier-Stokes Eq. (1), the diffusivity coefficient Γ is the effective viscosity defined by $\mu_{ef} = \mu_t + \mu_l$, where μ_t and μ_l are the turbulent and laminar viscosity, respectively.

BOUNDARY CONDITIONS

Typically, in an environmental flow we have as solid boundaries the shoreline and the bottom of the water body. At the surface the wind action will define the flow pattern in the water. For the solid and surface boundaries no normal flux of momentum is allowed. The turbulent stresses at the solid boundaries, σ_b , are determined by

$$\sigma_b = \frac{k_v\, v_b}{\ln\left(\dfrac{\Delta Z_b}{Z_0}\right)} \tag{3}$$

where v_b is the component of the velocity *parallel to the boundary*, k_v = 0.41 is the von Kármán constant, ΔZ_b the distance from the boundary to the nearest grid point and Z_0 a parameter dependent on the local boundary roughness (Jin [5]). Assuming hydraulically smooth flow Eq. (3) assumes that the velocity near the solid boundaries matches the logarithmic law of the wall. At the surface the wind stress is often calculated by (Huang and Spaulding, [6])

$$\tau_s = \rho_w C_w v_{wind}^2 \tag{4}$$

where C_d is the air-water drag coefficient, ρ_w the air density and v_{wind} is the wind velocity measured at 10 meters above the water level. The stresses at the boundary imposes the boundary conditions for the velocity as shown in Jucá and Maliska[7].

CLOSED CHANNELS UNDER SURFACE WIND ACTION: LAMINAR MODEL VERIFICATION

For channel flows as depict in Fig.1, the simplest case is when a laminar flow is imposed, and an analytical solution is possible. This problem, in spite of its simplicity, is an efficient test for the numerical model since a 3D grid is used for this case. Symmetry conditions are, therefore, also tested. The Navier-Stokes equations for this two-dimensional case is reduced to

$$\frac{\partial^2 u}{\partial^2 z} = 0 \tag{5}$$

under the boundary conditions

$$\mu\frac{\partial u}{\partial z} = \tau_s \quad \text{at} \quad z = D \tag{6}$$
$$u(z) = 0 \quad \text{at} \quad z = 0 \tag{7}$$

assuming that the wind stress is known. Taking into account the principle of mass conservation ($\int_0^D u(z)\,\partial z = 0$), the analytical solution is

$$u(z) = \frac{\tau_s}{4\mu D}\, z(3z - 2D) \tag{8}$$

If the surface velocity is known, instead of the stress, the boundary condition (6) changes to $u(z) = u_s$ for $z = D$, which leads to an alternative analytical solution to (5), given by

$$u(z) = \frac{u_s}{D^2}\, z(3z - 2D) \tag{9}$$

The two former solutions are based in the two possible surface boundary condition allowed for wind driven flows, that is, the velocity or the wind stress imposed at the surface. In general cases, based in field data, the wind velocity is known and the surface stress can be estimated by Eq. (4). If the flow is laminar, it is possible, using the former analytical solutions, determine the velocity that will impose the same flow pattern correspondent to a given stress. The relation between the velocity and stress for the same flow pattern is given by

$$\frac{\tau_s}{\mu} = 4\frac{u_s}{D} \tag{10}$$

or, taking the surface velocity friction definition,

$$u_{*s} = \left(\frac{\tau_s}{\rho}\right)^{0.5} = \left(4\frac{\mu\, u_s}{\rho D}\right)^{0.5} \tag{11}$$

This analysis is very useful to verify the mathematical model behavior when simulating laminar flows. Although, as stated before, the nature of wind driven flows in closed water bodies is turbulent, this is a good problem for testing the implementation and solution procedures.

The physical domain of 10.0m length, 2.30m wide and 0.50 depth was discretized by a 80x7x20 equally spaced mesh. As the present flow is 2D, symmetry boundary conditions were employed for the "y" direction, so the volume numbers in this direction is not relevant. Refer to Fig. 1 for the other boundary conditions.

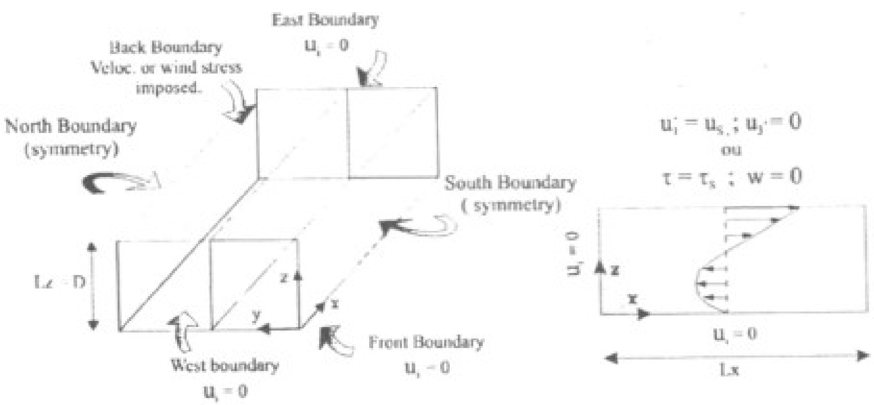

Figure1 - Two-dimensional flow in a closed channel

A low Reynolds number was choosen for this experiment to guarantee the laminar behavior. It is defined as

$$Re_s = \frac{\rho u_s D}{\mu_l} = 18{,}73 \qquad (12)$$

Fig. 2 compares the vertical velocity profiles for the analytical solution, Eq. (8) and (9), against the velocity profile predict by the numerical model. Both velocity and stress boundary conditions are compared and both show an excellent agreement.

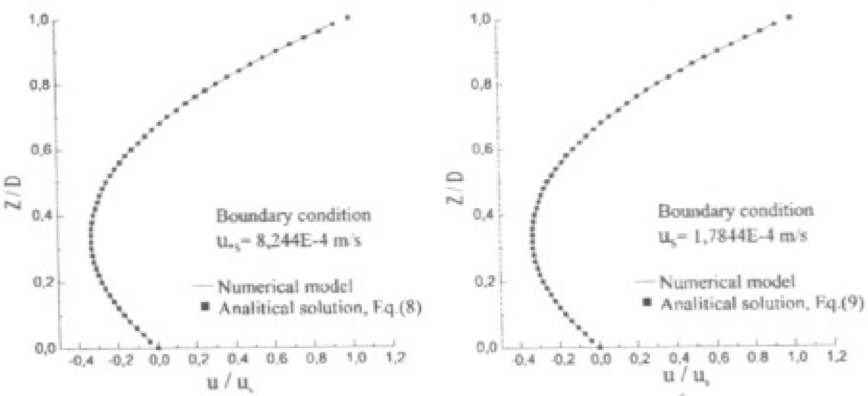

Figure 2 - Vertical velocity profile for laminar flow in a closed channel.

TURBULENT FLOWS: MODEL VERIFICATION

Tsanis [8] proposed a parabolic profile for the turbulent viscosity that leads to an analytical solution for the vertical velocity profile in 2D wind driven closed channels[9]. The solution proposed show good agreement with experimental measurements for these vertical velocity profiles. In this work this turbulent viscosity profile is implemented in to the numerical code as a algebraic turbulent model and the result is compared with experimental results in order to verify the accuracy of the numerical model.

The vertical turbulent viscosity profile, given by Tsanis [8] for 2D wind driven closed channels, is

$$\nu_t = \frac{\mu_t}{\rho} = \left(\frac{\lambda u_{*s}}{D}\right)(z + z_b)(D - z + z_s) \qquad (13)$$

where $u_{*s} = (\tau_s / \rho)^{0,5}$ is the surface friction velocity and λ a constant that characterizes the turbulence intensity. λ is given accordingly to the Reynolds number range as

$$10^3 \le \quad Rs = \frac{\rho u_s D}{\mu} \quad \le 10^5 \qquad 0{,}20 \le \lambda \le 0{,}50$$

The parameters z_b e z_s in Eq. (13) are characteristics lengths determined at the bottom (z = 0) and at the surface of the water body (z = D), respectively. They are a relative measure of the thickness of the viscous sublayers. Tsanis [10] found, through experimental studies, that their values should be taken as $z_{sh} = z_s/D = 2{,}20\times10^{-4}$ and $z_{bh} = z_b/D = 0{,}60 \times 10^{-4}$.

Based on the former viscosity profile, Wu and Tsanis [9] found an analytical solution for the velocity profile, normalized by the surface shear velocity, given by

$$\overline{u}(z) = \frac{u(z)}{u_{*s}} = A\ln\left[1 + (z/z_s)\right] + B\ln\left\{1 - \left[z/(z_b + D)\right]\right\} \qquad (14)$$

where $A = f_1(z_{sh}, z_{bh})$ and $B = f_2(z_{sh}, z_{bh})$, as can be seen in [9]. In the experimental works of Baines and Knapp [11] and Wu and Tsanis [9], both stress and velocity are available as experimental results, so both can be specified as boundary conditions. Therefore, these experimental works are well suited to check the mathematical model proposed. Table 1 resumes the experimental data related to these works.

Table 1 - Data and experimental results from Baines and Knapp [11]

Data	Symbol	Unit	Experiment A	Experiment B
Depth	D	m	0,3048	0,3048
Wind velocity	u_a	m/s	3,901	6,096
Friction velocity at the surface	u_{*s}	cm/s	0,6233	0,9416
Surface velocity	u_s	cm/s	10,72	15,25
Reynolds number	R_s	#	32700	46500
Normalized surface velocity	u_s/u_{*s}	#	17,2	16,2
Equivalent roughness height	z_{ob}	mm	0,3521	0,4795
Height of zero velocity	z_{v0}/D	#	0,69	0,68

The boundary conditions imposed to the model can be seen in Fig. 1. A vertical profile for μ_t, following Eq. (13), using the friction velocity listed in Table 1 was used. The physical domain, as in the experiment, was Lx = 2,4 m , Ly = 0,72 and Lz = D = 0,3048. As stated before two kinds of boundary conditions may be imposed at the surface and bottom boundaries. Table 2 resumes these conditions.

Table 2 - Boundary conditions at surface and bottom

Boundary	Case A	Case B
Surface	Velocity: $u = u_s$	Stress: $u_{*s} = u_{*s}$ (experim.)
Bottom	Velocity: $u = 0$	Stress: u_{*b} = Eq.(3)

The bottom friction velocity can be calculated once the equivalent roughness height is available as a experimental data (Jin, [5]) using Eq.(3) with $z_0 = z_b$. During the numerical solution procedure this friction velocity must be updated because the velocity in Eq.(3) is the one available in the last iterative step. When the solution is achieved, the velocity field no longer changes and so the friction velocity. Based on previous laminar simulation an equally spaced mesh of 80x7x20 volumes (x,y,z directions) was employed.

The resulting vertical velocity profiles, using both boundary conditions for Experiment A, Table 1, (Re = 32700), is show in Fig.3 where is also shown the analytical solution. For Eq. (19) the values of λ , z_{sh} e z_{bh} , as recommended by [9], where 0.35; 2.2 x 10^{-4} e 1.4 x 10^{-4} respectively.

The resulting velocity profiles fits well the analytical solution in the central core of the channel. But near the boundaries the profiles are not in good agreement. The B case boundary condition is somewhat better near the surface but near the bottom the result is even worse. Taking u_s / u_{*s} as a parameter to compare the correctness of the solution near the surface the results are not so good as showed in Table 3.

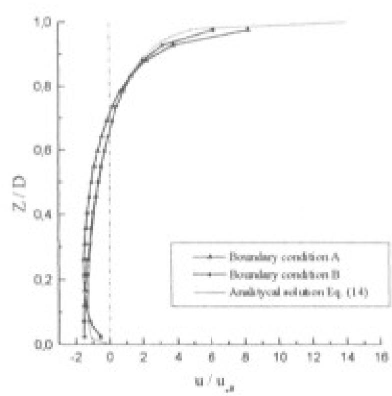

Figure 3- Velocity profiles for a closed channel flow (boundary condition A: normalized by u_{*s} = 0,8893; boundary condition B: normalized by u_{*s} = 0,6233).

Table 3 - Numerical values of u_s / u_{*s}

Boundary Condition	u_s / u_{*s}	Cause
A	12,1	Surface stress not well solved by the numerical model
B	8,92	Velocity profile near the surface not well solved by the numerical model
Experimental	17,2	#

What we learn from these results is that if the focus is in the bulk flow, the

data available is the wind velocity, wich allows the calculation of the friction velocity through Eq.(4). In the other hand if the dispersion of a floating pollutant or the bottom erosion is the main focus, the velocity profile must have a better solution near these boundaries. To improve the numerical solution near the boundaries the mesh needs fine resolution.

Fig.4 shows the vertical velocity profiles for meshes of 21 and 41 equally spaced volumes in "z" direction and for one mesh 40 "z" direction volumes equally concentrated near the surface and bottom boundaries. All cases employed the boundary condition of A kind. As expected, the bulk flow solution is practically the same in all cases, but the profiles near the boundaries are somewhat better as in the previous case. Also the u_s / u_{*s} parameter confirm this improvement in the solution as shown in Table 4.

Fig.5 compares the vertical velocity profiles for the 40 "z" direction volumes equally concentrated mesh with "A" boundary condition, with the experimental velocity profiles reported by Baines and Knapp [11]. The agreement with the experimental velocity profiles is very good, except near the bottom. However, it should be noted that the distinct peak exhibited in the experimental return flow near the bottom are reported by the authors to be due to the short length of the experimental channel and the presence of a sloping bank at its end. Detailed currents had not been measured close to the bottom, lower than 10% of the whole depth. Taking it into account we could conclude that the numerical model is able to correct simulate the wind driven flows in closed channels.

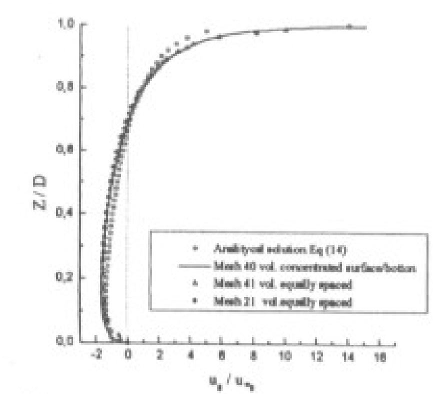

Figure 4 - Effects of the mesh resolution and distribution over the velocity profiles

Table 4 - Values of u_s / u_{*s} for different meshes

Mesh ("z" direction)	u_s / u_{*s}
21 volumes equally spaced	12.01
41 volumes equally spaced	13.33
40 volumes, surface/bottom concentrated	16.18
Experimental	**17,2**

CONCLUSIONS

This paper presented part of a systematic procedure for evaluating a full three-dimensional turbulent model developed for predicting environmental flows with buoyancy effects. The profile for two approach of applying boundary conditions at the surface of water body and at the bottom, demonstrated that the treatment of the turbulence near the walls is producing physically realistic results. Although the results shown here report only 2D flows, the model developed can solve fully 3D flows in water bodies with complex shapes. Future papers will report the model evaluation in these situations.

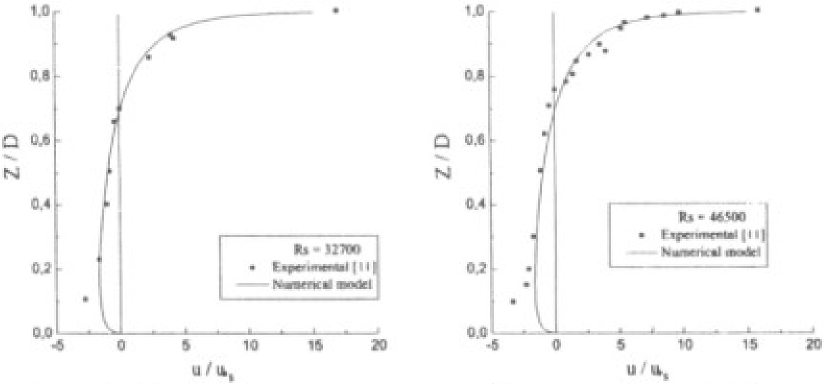

Figure 5 - Vertical velocities profiles: numerical and experimental [11] results.

REFERENCES

1. Rodi, W., Turbulence Models and Their Application in Hydraulics, Int. Assoc. for Hydraulic Research , Delft, Netherlands, 1980.

2. Maliska, C.R., Transferência de Calor e Mecânica dos Fluidos Computacional: Fundamentos e Coordenadas Generalizadas, Livros Técnicos e Científicos Editora, 1995

3.Van Doormaal, J.P., Raithby, G.D., Enhancements of the SIMPLE Method for Predicting Incompressible Fluid Flow, Num. Heat Transfer, vol. 7 pp. 147-163, 1984

4. Jucá, P.C.S., Modelagem Tridimensional Turbulenta da Dispersão de Poluentes em Corpos D'água de Geometria Variável, Exame de Qualificação do Curso de Pós-graduação em Engenharia Mecânica, UFSC, Centro Tecnológico; Universidade Federal de Santa Catarina, 1994

5. Jin, X.Y., Quasi-Tridimensional Numerical Modeling of Flow and Dispersion in Shallow Water, Communication on Hydraulic and Geotechnical Engineering, Dp of Civil Eng., Delft Univ. of Technology, Rep. 93-03, ISSN 0169-6548, 1993

6. Huang, W., Spaulding, M., 3D Model of Estuarine Circulation and Water Quality Induced by Surface Discharges, Journal of Hydraulic Eng., vol. 121, No 4, pp. 300-311, 1995

7. Jucá, P.C.S. , Maliska, C.R., Turbulent Water Channel Flows under Surface Wind Action, VI Congresso Brasileiro de Engenharia e Ciências Térmicas/VI Congresso Latinoamericano de Tranferencia de Calor y Materia, pp 383-388, Florianópolis, SC, Brasil, 1996

8. Tsanis, I. K. , Simulation of Wind-Induced Water Currents, Journal of Hydraulic Engineering, vol. 115, No. 8, August, pp 1113-1134, 1989

9. Wu, J, Tsanis, I.K., Numerical Study of Wind-Induced Water Currents, Journal of Hydraulic Engineering, May, pp 388-395, 1995

10. Tsanis, I. K., The Structure of Turbulent Shear-induced countercurrent Flow, Journal of Fluid Mechanics, vol 189, pp 531-552, 1988

11. Baines, W.D., Knapp D., Wind Driven Water Currents, Hydraulic Division, Proceedings of the American Society of Civil Engineers, vol. 91, March, pp 205-221, 1965